A combined biomaterial and cellular approach for annulus fibrosus rupture repair

Tatiana Pirvu, Sébastien B.G. Blanquer, Lorin Benneker, Dirk Grijpma, Robert I. Richards, Mauro Alini, David Eglin, Sibylle Grad, Zhen Li

A combined biomaterial and cellular approach for annulus fibrosus rupture repair

Tatiana Pirvu [a, e], Sebastien B.G. Blanquer [b, e], Lorin M. Benneker [c, e], Dirk W. Grijpma [b, d, e], Robert G. Richards [a, e], Mauro Alini [a, e], David Eglin [a, e], Sibylle Grad [a, e], Zhen Li [a, e, *]

[a] *AO Research Institute Davos, Davos 7270, Switzerland*
[b] *MIRA Institute for Biomedical Technology and Technical Medicine, Department of Biomaterials Science and Technology, University of Twente, AE Enschede 7500, The Netherlands*
[c] *Department of Orthopaedic Surgery, University of Bern, Bern 3010, Switzerland*
[d] *University of Groningen, University Medical Center Groningen, W.J. Kolff Institute, Department of Biomedical Engineering, AD Groningen 9700, The Netherlands*
[e] *Collaborative Research Partner Annulus Fibrosus Repair Programme, AO Foundation, Davos 7270, Switzerland*

ARTICLE INFO

Article history:
Received 24 September 2014
Accepted 25 November 2014
Available online 10 December 2014

Keywords:
Annulus fibrosus rupture repair
Poly(trimethylene carbonate) scaffold
Poly(esterurethane) membrane
Mesenchymal stromal cells
Implantation

ABSTRACT

Recurrent intervertebral disc (IVD) herniation and degenerative disc disease have been identified as the most important factors contributing to persistent pain and disability after surgical discectomy. An annulus fibrosus (AF) closure device that provides immediate closure of the AF rupture, restores disc height, reduces further disc degeneration and enhances self-repair capacities is an unmet clinical need. In this study, a poly(trimethylene carbonate) (PTMC) scaffold seeded with human bone marrow derived mesenchymal stromal cells (MSCs) and covered with a poly(ester-urethane) (PU) membrane was assessed for AF rupture repair in a bovine organ culture annulotomy model under dynamic load for 14 days. PTMC scaffolds combined with the sutured PU membrane restored disc height of annulotomized discs and prevented herniation of nucleus pulposus (NP) tissue. Implanted MSCs showed an up-regulated gene expression of type V collagen, a potential AF marker, indicating *in situ* differentiation capability. Furthermore, MSCs delivered within PTMC scaffolds induced an up-regulation of anabolic gene expression and down-regulation of catabolic gene expression in adjacent native disc tissue. In conclusion, the combined biomaterial and cellular approach has the potential to hinder herniation of NP tissue, stabilize disc height, and positively modulate cell phenotype of native disc tissue.

1. Introduction

Intervertebral disc (IVD) herniation affects mostly the young working population with a mean lifetime prevalence of 1e3% [1], which leads to a high socioeconomic burden [2]. As a standard surgical treatment for disc herniation, herniotomy or partial discectomy leaves the annulus fibrosus (AF) ruptured, while complete discectomy even creates further invasion. Despite acceptable rates of success in relieving pain and improving function, 20e25% of discectomy patients continue to experience unsatisfactory outcome [3], with recurrent disc herniation as one of the most important factors of discomfort. It has been reported that large annular defects are associated with an increased rate of reherniation [4,5], which suggests that repair of ruptured AF would be indicated in case of large disc protrusion.

Several attempts have been made to mend the AF defect with a suture after discectomy; however, outcomes have been inconsistent. Suture of ruptured AF reduced the reherniation risk in patients with predominant leg pain before discectomy, but did not significantly affect the overall reherniation rate [6]. In a porcine model, sutured discs resisted repeated compression forces *ex vivo* and showed less degenerative changes compared with unrepaired discs *in vivo* [7]. However, in an *in vivo* study in sheep, suture of AF incisions did not significantly improve the healing strength after discectomy [8]. Biomechanical tests further suggested that suture alone is not sufficient for long-term reliable AF closure [9]. Glues based on natural polymers, such as high-density collagen gel [10] and fibrin-genipin glue [11], are only capable of repairing small annular defects. The

* Corresponding author. AO Research Institute Davos, Clavadelerstrasse 8, 7270 Davos, Switzerland. Tel.: þ41 81 414 2318; fax: þ41 81 414 2288.
E-mail address: zhen.li@aofoundation.org (Z. Li).

functional mechanical property of the AF tissue is essentially determined by the components and structure of the biological matrix. Taken together, the results of previous studies indicate the need for a combined mechanical and biological repair to restore the mechanical and biological integrity in large AF defects.

Tissue engineering approaches aiming for structural and biological AF repair have also been investigated in the last decade [12e14]. It has been suggested that the optimum AF tissue engineering scaffold should reproduce the structure and the mechanical properties of the native AF tissue [15]. Recently we developed poly(trimethylene carbonate) (PTMC) scaffolds prepared by stereolithography with identical interconnected architecture and different pore sizes that are suitable for culture of AF cells *in vitro* [16]. The remarkable flexible and elastic properties of PTMC scaffolds enables us to obtain mechanical properties similar to native AF tissue which make them promising bioresorbable constructs for a tissue engineering approach [16].

In addition to a scaffold which should match the mechanical property of native AF tissue, a proper fixation method to maintain the scaffold within the AF defect under dynamic load is required [17]. An elastic poly(ester-urethane) (PU) membrane has been shown to support AF cell growth and function in our previous study [18]. In the current study, this membrane was used as a patch sutured onto the adjacent AF tissue to maintain the PTMC scaffold within AF defect.

The low functional cell density is known as a limiting factor in regenerative strategies [19,20]. Supplementation of cells may therefore accelerate the regeneration process of large annular defects. Differentiated AF cells have been studied as potential cell source for AF tissue engineering approaches [21]. However, the availability of functional autologous AF cells is highly limited. Mesenchymal stromal cell (MSC) transplantation therefore becomes an attractive alternative. MSC sheets attached to silk scaffolds [22], and MSCs embedded in electrospun nanofibrous scaffolds [23,24] are two reported strategies for generating engineered AF tissue. MSCs seeded in biphasic constructs have also shown potential for tissue engineering of biological IVD replacements [25]. Yet, these studies were conducted under *in vitro* conditions lacking the native disc microenvironment. In addition, most studies were performed in a static culture system without mechanical load. Evaluation of scaffolds and cell therapy under physiologically relevant loading condition is essential to reveal the advantages and limitations for clinical application.

The current study therefore combined mechanical and biological repair in a whole organ AF defect model under dynamic load. The combination of biomaterial, cell therapy, and implant fixation method for annulus fibrosus rupture repair under physiologically relevant assessment condition (organ culture and dynamic load) has been firstly developed in this study. Specifically, MSC-seeded PTMC scaffolds, sealed with a PU membrane via suture with the adjacent AF tissue were evaluated. The aims of this study were (1) to investigate the mechanical compatibility of the PTMC scaffold-PU membrane construct for AF defect closure *in situ* under dynamic load, and (2) to investigate the effect of MSC implantation on AF regeneration *in situ* under dynamic load.

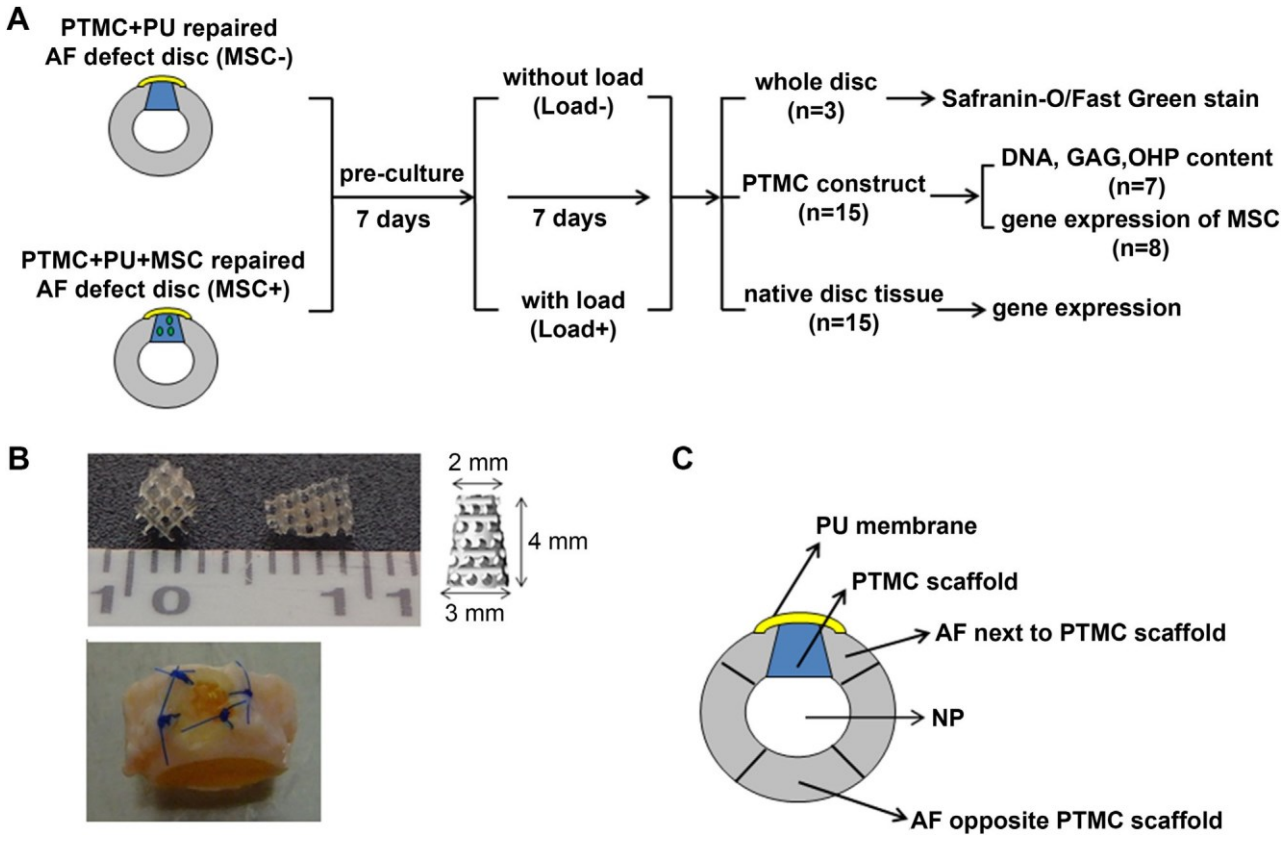

Fig. 1. (A) Schematic description of experimental procedure to assess PTMC scaffold-PU membrane-MSC constructs for large AF defect repair in organ culture system. (B) Macroscopic view of PTMC scaffold (top), and AF defect disc repaired with PTMC scaffold and sutured PU membrane (bottom). (C) Transverse schematic view of discs implanted with PTMC scaffold-PU membrane constructs and disc tissue collected for gene expression analysis.

2. Materials and methods

2.1. Fabrication of PTMC scaffolds

The PTMC scaffolds with AF mimicking pore architecture and truncated cone geometry were prepared by stereolithography (Fig. 1B top, diameter 2 and 3 mm, length 4 mm, pore size 420 μm and porosity ≥ 80%). The PTMC macromer used for the fabrication of the scaffolds was synthesized in two steps. The first step consists of ring opening polymerization of trimethylene carbonate monomer (0.98 mol, 100 g) in presence of stannous octanoate (0.05 wt%) and 1,1,1-Tris(hydroxymethyl)propane (TMP) (0.02 mol, 2.62 g) under stirring for 3 days at 130 °C in argon atmosphere, to reach a PTMC oligomer with an average molecular weight (Mn) of around 5000 g/mol. The end-functionalization by methacrylate groups is performed by reaction of the PTMC oligomer in solution in dichloromethane (100 mL) with methacrilic anhydride (0.18 mol; 26 mL) in presence of triethylamine (0.18 mol; 26 mL) at room temperature under argon atmosphere for 5 days. The macromers were purified by drop-wise precipitation in methanol and dried under vacuum over 3 days. Proton nuclear magnetic resonance (^{1}H-NMR, 300 MHz) was used to determine the conversion rate and the Mn of the macromers as well as the end-functionalization ratio. Finally the resin used with the stereolithograph was prepared by mixture of photo-initiator, such as Lucirin TPO-L (5 wt%) and Orasol Orange dye (0.15 wt%), with 30% of polypropylene carbonate. Once the resin was prepared, the scaffolds were built using an UV stereolithograph apparatus (EnvisionTech Perfactory MiniMultilens) at a pixel resolution of 16 × 16 mm^2 and a layer thickness of 100 μm. The irradiation time for solidifying each layer was fixed at 20 s for a light intensity of 180 mW/m^2. The scaffolds were purified by acetone extraction twice and dried stepwise in ethanol. As reported in a previous study, the compression modulus of the PTMC scaffolds is around 0.2–0.3 MPa, which is similar to the modulus measured from native AF tissue [16].

2.2. Fabrication and characterization of PU membrane

The PU was synthesized using a one-step solution polycondensation [26]. The monomers and macromers used for the synthesis were 1,6-hexamethylene diisocyanate (HMDI) (Sigma, Milwaukee, WI), a hydroxyl-terminated poly(ε-caprolactone) (PCL) (Aldrich, Milwaukee, WI) with a number average molecular weight of 530 g/mol and a functionality of 2 and 1,4,3,6-Dianhydro-D-sorbitol (ISO) (Aldrich, Milwaukee, WI). The HMDI:PCL:ISO molar ratio used was kept at 1:0.32:0.64. The PU intrinsic viscosity, weight average molecular weight and polydispersity measured were 1.3 dl/g, 500,000 g/mol and 2.00, respectively. The preparation of PU membrane was performed as follows: 15 g of PU were dissolved in 150 mL of *N*,*N*-dimethylformamide (DMF) (Fluka, Buchs, CH) overnight with strong magnetic stirring at RT. Then, 150 mL of tetrahydrofuran (THF) (Fluka, Buchs, CH) and 80 mL of acetone (Fluka, Buchs, CH) were added and the mixture stirred until a completely transparent solution was obtained. 60 mL of the solution was poured in glass petri-dishes (19 cm diameter, flat bottom). The petri-dishes were placed on a flat table under a chemical fume-hood, covered with a polypropylene porous sheet and left for drying at RT for 4 days. At this time, ethanol (99%, Fluka, Buchs, CH) was poured onto the petri-dishes. After three ethanol washing steps of at least 1 h, the membranes were collected and left to dry slowly in air for 2 days before a second drying under vacuum for at least 2 days. PU membrane discs were cut at diameter of 6 mm.

To characterize the mechanical property of the membrane, strip-shaped specimens were prepared by cutting larger membrane samples. Tests were performed on the dry samples using an Instron mechanical testing system model 4302 (High Wycombe, Bucks, UK) equipped with a 100 N load cell at room temperature (20 °C), with a relative humidity of around 25% and atmospheric pressure. A strain rate of 10 mm min^{-1} was used to test 7 replicate samples. The ultimate and yield strength values (MPa) as well as the elongation at break (%) were deduced from the tensile curves.

The PU membrane surface and cross-section after cryo-fracture were imaged by scanning electron microscopy (SEM) using an S-4100 field emission microscope (Hitachi, Tokyo, Japan). Samples were coated directly with a 10 nm gold/platinum layer and imaged in secondary electron (SE) mode with the instrument operated at 5.0 kV and 40 mA.

2.3. Isolation and expansion of human bone marrow derived MSCs

Bone marrow aspirates were obtained with ethical approval from the Swiss cantonal authorities (KEK 188/10) and informed consent. Mononuclear cells from bone marrow were collected with Ficoll (Sigma–Aldrich, St. Louis, USA) cushion as previously described [27]. The isolated cells were plated in polystyrene cell culture flasks, supplemented with αMEM (Gibco, Paisley, UK), 10% fetal calf serum (FCS, Gibco, Paisley, UK), and 5 ng/mL recombinant human basic fibroblast growth factor (Fitzgerald, Acton, USA), and cultured at 37 °C, 5% CO_2, 85% humidity. The medium was changed after 4 days, and afterward 3 times weekly. Passage 2 (P2) MSCs from 6 donors (4 female, 2 male, age 18–49 years) were used in the current study.

2.4. Intervertebral disc dissection

Caudal IVDs were harvested from seventeen 6–9 months old calves obtained from a local slaughterhouse within three hours of death. Whole discs with endplates (EPs) were isolated using a band saw [28]. EP surfaces were cleaned with Ringer's balanced salt solution suing a Pulsavac Wound Debridement Irrigation System (Zimmer, Minneapolis, USA) to remove cutting debris and blood clots. IVDs were then cultured in DMEM supplemented with 100 units/mL penicillin, 100 mg/mL streptomycin (all products from Gibco, Paisley, UK), 10% FCS, 50 mg/mL ascorbate-2-phosphate (Sigma Aldrich, St. Louis, USA), and 100 mg/mL primocin (Invitrogen, San Diego, CA, USA) at 37 °C, 85% humidity and 5% CO_2.

2.5. MSC seeding into PTMC scaffold

The PTMC scaffolds were pre-wetted in DMEM in vacuum for 1 h. Before cell seeding, the medium was aspirated completely from the scaffolds. P2 MSCs were trypsinized, suspended in 15 mL fibrinogen solution at a cell density of 0.2 × 10^6 per scaffold and mixed with 15 mL thrombin solution, resulting in a final concentration of 9 × 10^6 cells/cm^3 in scaffold. The PTMC scaffold was immediately pressed into the cell-fibrin-suspension, released to let the suspension infiltrate, and incubated at 37 °C for 45 min for gellification. The fibrin components were provided by Baxter Biosurgery (Vienna, Austria). The final concentrations of the fibrin components were 17 mg/mL fibrinogen and 0.5 units/mL thrombin. For implants without MSCs, pure fibrin gel was infiltrated into the PTMC scaffolds.

2.6. Implantation of PTMC scaffolds into IVDs

The experimental set-up is shown in Fig. 1A. MSCs from 6 independent donors were implanted into bovine caudal discs from 18 independent calves separately (3 calves replicates per MSC donor). Discs from 3 calves seeded with MSCs from 3 different donors were evaluated by Safranin O/Fast Green staining. Implanted scaffolds and native disc tissue from the other 15 calves were evaluated for biochemical and gene expression analysis. From the implanted scaffolds, 8 scaffolds (1-2 calves replicates per MSC donor, from 6 independent MSC donors) were used for gene expression measurement of MSCs; 7 scaffolds (1-2 calves replicates per MSC donor, from 6 independent MSC donors) were used for biochemical analysis. Native disc tissue from 15 calves (2-3 calves replicates per MSC donor, from 6 independent MSC donors) were evaluated for gene expression analysis.

Using a biopsy punch (diameter 2 mm, depth 7 mm; Kai Medical Europe GmbH, Solingen, Germany), a defect was created through the AF of the bovine caudal discs, and complete annulotomy was performed. The PTMC scaffold with or without seeded MSCs (3 mm end towards NP, 2 mm end towards outside) was press-fitted into the AF cavity. The defect was then covered with a PU film sutured (4 point-suture) with the surrounding AF tissue using a 5-0 Prolene (Ethicon, Somerville, NJ, USA) (Fig. 1B bottom).

IVDs were cultured for 2 weeks in DMEM, 1% P/S, 1% non-essential amino acid (Gibco, Paisley, UK), 50 mg/mL ascorbate-2-phosphate, 1% ITS+ (Cell Culture Supplement, 100×, BD Biosciences, Bedford, MA, USA), 10^{-7} M dexamethasone (Sigma Aldrich, St. Louis, USA), 2% FCS, 50 mg/mL primocin. The medium was changed daily and collected for glycosaminoglycan (GAG) and orthohydroxyproline (OHP) quantification.

2.7. Dynamic loading of IVDs and disc dimension measurement

After one week of free swelling pre-culture, dynamic load was applied on the IVDs using a custom-made bioreactor system [29]. The loading protocol consisted in 3 h of sinusoidal dynamic load per day for 7 consecutive days, at 0–0.1 MPa, 0.1 Hz. In between the dynamic loading periods, discs were cultured free swelling in 6-well plates. Non-loaded samples served as controls and were cultured free swelling in 6-well plates.

Disc height was measured immediately after disc dissection (day 0), after 1 week of pre-culture (day 7), after 1st cycle of dynamic load (day 8) and 1st free swelling recovery overnight (day 9), and after 7th cycle of dynamic load (day 14) and 7th free swelling recovery overnight (day 15) respectively. Each disc was measured at 2 positions for disc height and the average value was used to calculate percentage of disc height change normalized to the initial dimension after dissection.

2.8. Safranin-O/Fast Green staining

The extracellular matrix deposition within the PTMC scaffolds and the native tissue was qualitatively evaluated by Safranin-O/Fast Green staining. After 14 days of culture, IVDs were fixed in 70% methanol and transferred into PBS with 5% sucrose at 4 °C overnight before cryosectioning. Transverse sections of IVDs were made at a thickness of 12 μm. Sections were stained with 0.1% Safranin-O and 0.02% Fast Green to reveal proteoglycan and collagen deposition respectively, and counterstained with Weigert's Haematoxylin to reveal cell distribution.

2.9. Gene expression of implanted MSCs and native disc cells

Gene expression analysis of human MSCs in PTMC scaffolds (n = 8/group) and native disc tissue (n = 15/group) was performed after 14 days of culture. AF tissue adjacent and opposite to the PTMC scaffold, as well as nucleus pulposus (NP) tissue (70–100 mg/sample) were collected (Fig. 1C), placed in RNA later (Sigma–Aldrich, St. Louis, USA) at 4 °C overnight and then stored at −20 °C. Samples were snap-frozen in liquid nitrogen and homogenized within 1 mL TRI reagent and 5 mL

Table 1
Oligonucleotide primers and probes used for real time PCR.

Bovine COL1A2	Primer fw (5′e3′)	TGC AGT AAC TTC GTG CCT AGC A
	Primer rev (5′e3′)	CGC GTG GTC CTC TAT CTC CA
	Probe (5′FAM/3′TAMRA)	CAT GCC AAT CCT TAC AAG AGG CAA CTG C
Bovine COL2A1	Primer fw (5′e3′)	AAG AAA CAC ATC TGG TTT GGA GAA A
	Primer rev (5′e3′)	TGG GAG CCA GGT TGT CAT C
	Probe (5′FAM/3′TAMRA)	CAA CGG TGG CTT CCA CTT CAG CTA TGG
Bovine ACAN	Primer fw (5′e3′)	CCA ACG AAA CCT ATG ACG TGT ACT
	Primer rev (5′e3′)	GCA CTC GTT GGC TGC CTC
	Probe (5′FAM/3′TAMRA)	ATG TTG CAT AGA AGA CCT CGC CCT CCA T
Bovine MMP13	Primer fw (5′e3′)	CCA TCT ACA CCT ACA CTG GCA AAA G
	Primer rev (5′e3′)	GTC TGG CGT TTT GGG ATG TT
	Probe (5′FAM/3′TAMRA)	TCT CTC TAT GGT CCA GGA GAT GAA GAC CCC
Bovine GAPDH	Primer fw (5′e3′)	GGC TGC TTT TAA TTC TGG CAA A
	Primer rev (5′e3′)	AAT CAT ACT GGA ACA TGT AGA CCA TGT A
	Probe (5′FAM/3′TAMRA)	TGG ACA TCG TCG CCA TCA ATG ACC
Human ACAN	Primer fw (5′e3′)	AGTCCTCAAGCCTCCTGTACTCA
	Primer rev (5′e3′)	CGGGAAGTGGCGGTAACA
	Probe (5′FAM/3′TAMRA)	CCGGAATGGAAACGTGAATCAGAATCAACT

polyacryl carrier (both Molecular Research Centre Inc., Cincinnati, OH, USA) using a tissue-lyser (Retsch GmbH & Co., Haan, Germany). RNA isolation was carried out according to the manufacturer's protocol. Reverse transcription was performed using SuperScript® VILO™ cDNA Synthesis Kit (Invitrogen) and 500 ng of total RNA according to the manufacturer's protocol.

StepOnePlus™ System (Applied Biosystems) was used to conduct quantitative real-time polymerase chain reaction (qRT-PCR). Gene expression of bovine collagen type I (COL1A2) and type II (COL2A1), aggrecan core protein (ACAN), and matrix-metallo-proteinase 13 (MMP13) in disc cells was analyzed using custom designed primers and TaqMan probes (Microsynth, Switzerland, Table 1). It was verified that no human MSCs were present in the disc tissue samples collected for RNA extraction. For human MSCs within PTMC scaffolds, gene expression of human ACAN (Microsynth, Switzerland, Table 1) and collagen type V (COL5A1, Hs00609088_m1, Applied Biosystems) was analyzed. The human primers and probes used in this study have been verified to not cross react with bovine cells. Relative quantification of target mRNA was performed according to the comparative C_T method with bovine glyceraldehyde 3-phosphate dehydrogenase (GAPDH, Microsynth, Switzerland, Table 1) and human GAPDH (4326317E, Applied Biosystems) as endogenous controls for bovine disc cells and human MSCs respectively.

2.10. Biochemical analysis of PTMC scaffolds and medium

After 14 days of culture in IVDs, PTMC constructs were removed from IVDs and placed in 0.5 mg/mL proteinase K solution (Roche, Mannheim, Germany) overnight at 56 °C (n ¼ 7/group). DNA content was measured spectrofluorometrically by Hoechst 33258 assay (Polysciences Inc., Eppelheim, Germany) using calf thymus DNA (Invitrogen, LuBioScience) as standard [30].

GAG content in proteinase K digested PTMC constructs (n ¼ 7/group) and conditioned media samples (n ¼ 15/group) was quantified using dimethylmethylene blue assay (1.9-DMMB, Sigma Aldrich) [31]. OHP content of PTMC constructs and conditioned culture media was determined as described elsewhere [18].

2.11. Statistical analysis

SPSS 21.0 statistical software was used for statistical analysis. Data were confirmed to be normally distributed using one-sample KolmogoroveSmirnov test (normal distribution at $p > 0.1$), including disc height, DNA, GAG, gene expression of MSCs, and gene expression of AF and NP tissue after removing outliers. For gene expression data of MSCs and disc tissue, 2^{-DDCt} values were used to determine differences among groups on day 14, and DCt values were used to determine differences between day 0 and day 14. One-way ANOVA Tukey *post hoc* test was used to determine differences among four groups. Independent 2 tailed T-test was used to determine differences between two groups. $p < 0.05$ was considered statistically significant.

3. Results

3.1. Characterization of PU membrane

The ultimate strength of the PU membrane was 53.0 ± 2.0 MPa, the yield strength was 4.9 ± 1.4 MPa and the elongation at break was 593.8 ± 57.7%. The surfaces of the PU membrane did not present large porosity and was mostly smooth on the top and bottom (Fig. 2A). Similarly, cross-section SEM image showed the absence of large pores and only minor amount of non-connected microporosity (Fig. 2B).

3.2. Disc height change

To assess the effect of the PTMC scaffold-PU membrane construct with suturing on disc height, defect only discs and intact discs served as negative and positive controls. Following 1 week of pre-culture, the disc height increased by 2.2 ± 0.8% for defect only discs, 4.1 ± 1.3% for intact discs, and 4.9 ± 1.2% for AF repaired discs compared with disc heights immediately after dissection (Fig. 3). On day 8 after 1st cycle of dynamic load, a disc height loss compared with the initial dimension was noticed in all discs, with defect only discs having the greatest disc height loss of –15 ± 0.6%, followed by AF repaired discs (–11 ± 1.6%) and intact discs (–9.0 ± 0.9%). On day 9 after free swelling, all the discs recovered to the level before load (increase by 0.7 ± 1.3% for defect only discs, 2.6 ± 1.8% for intact discs and AF repaired discs without MSCs, 3.6 ± 1.2% for AF repaired discs with implanted MSCs compared with initial dimension). On day 14 after 7 repetitive dynamic load cycles, discs showed the same trend as on day 8 after 1st dynamic load cycle, with an additional –2% of further disc height loss. On day 15 after free swelling recovery, defect only discs showed significantly lower disc height compared with the same discs on day 7 before applying repetitive dynamic load ($p < 0.001$), which indicates that defect discs loose height by time. In contrast, intact

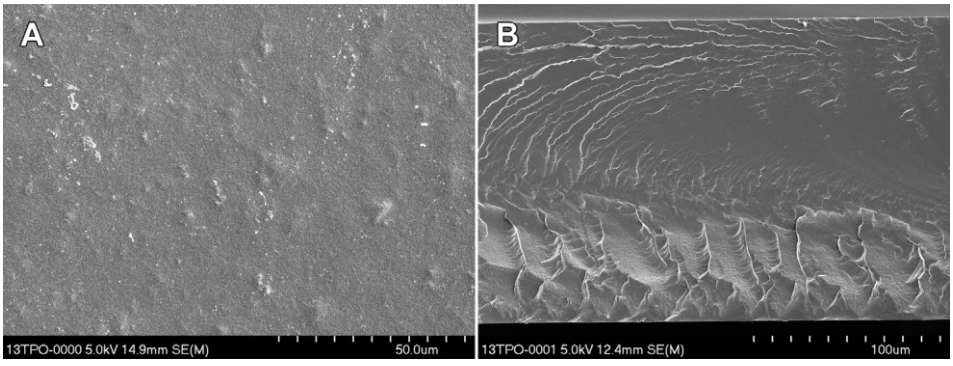

Fig. 2. Representative SEM images of the PU membrane surface (A) and cross-section (B).

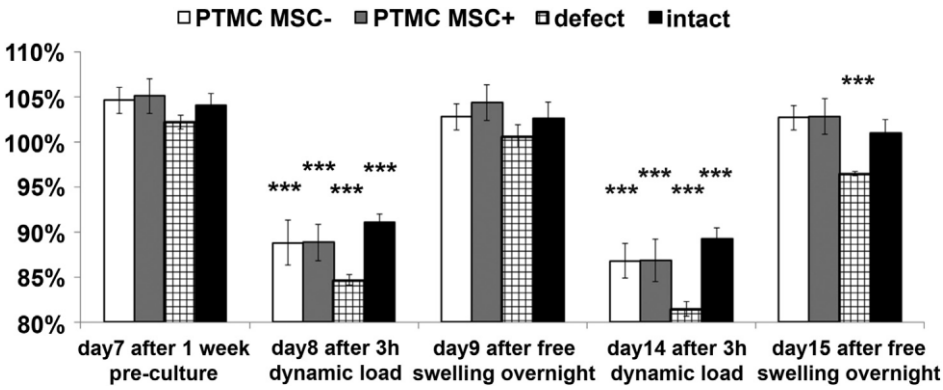

Fig. 3. Disc height relative to initial dimension after dissection (day 0) at different time points: on day 7 after one week of pre-culture, day 8 after 3 h dynamic load, day 9 after free swelling overnight, day 14 after 3 h dynamic load, and day 15 after free swelling overnight. Discs with untreated defect and intact discs served as negative and positive controls. Mean ± SEM, n ¼ 18, ***$p < 0.001$ vs same group on day 7 before applying repetitive dynamic load.

discs and AF repaired discs retained disc heights comparable with day 7, which indicates that the disc height loss could be prevented by implanting scaffolds. There was no difference between discs with and without implanted MSCs.

3.3. Histological analysis of whole IVDs

Safranin O/Fast Green stained sections of annulotomized discs revealed that NP tissue pushed out of its normal space and herniated into the AF defect after 14 days of culture (Fig. 4A, B). In annulotomized discs repaired with PTMC scaffolds and sutured PU membrane, the NP tissue was maintained in its normal space by the implant and the PTMC scaffolds remained within the AF defect without dislocation after repetitive dynamic load (Fig. 4C, D).

Higher magnification images are shown in Fig. 5, where "f" indicates fibrin gel, "s" indicates PTMC scaffold fiber, and "t" indicates native disc tissue. After 14 days of culture, fibrin gel without encapsulation of MSCs showed a mesh like structure (Fig. 5A and C). After encapsulation of MSCs, the implanted cells were still present in the fibrin gel after 14 days of culture with or without repetitive dynamic load (Fig. 5B and D). Besides, the fibrin gel adopted a wave like structure similar to native disc tissue. The fast green stain of implant areas was also more intense in MSCs implanted discs (Fig. 5B and D vs. A and C). Under free swelling culture condition, implanted MSCs appeared as compact clusters within the fibrin gel (Fig. 5B). Under repetitive dynamic load, implanted MSCs were more evenly distributed in the fibrin gel (Fig. 5D).

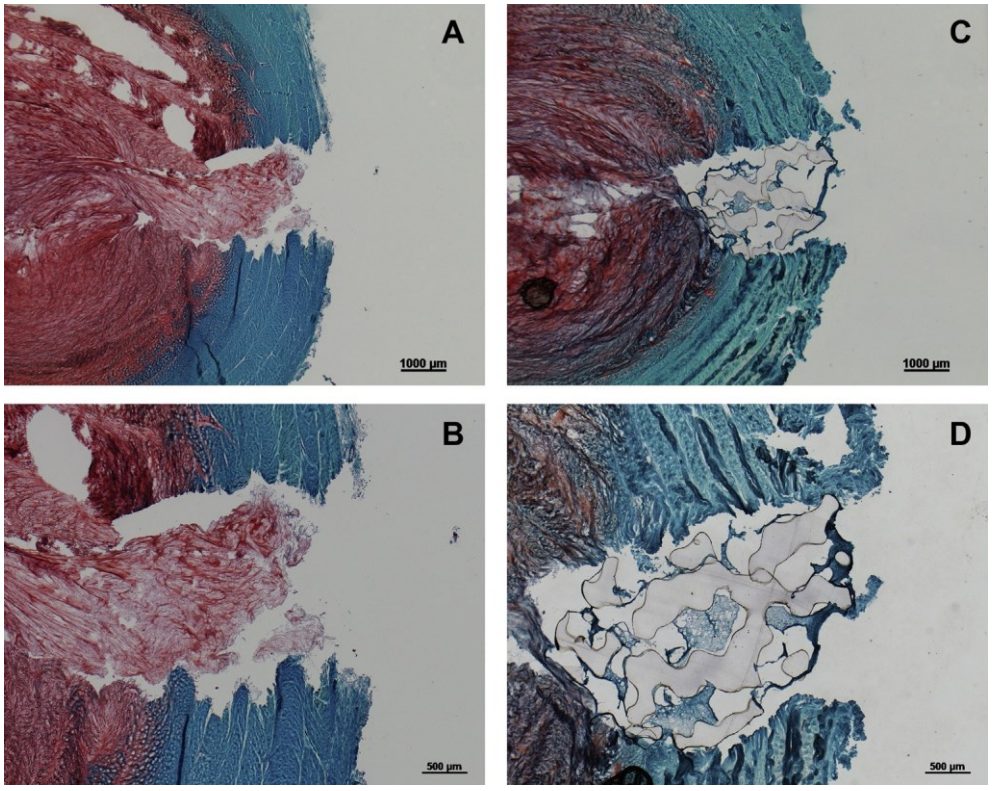

Fig. 4. Representative Safranin O/Fast Green stained sections of annulotomized discs (A, B) and annulotomized discs repaired with MSCs encapsulated PTMC scaffold and PU membrane (C, D) cultured for 14 days with dynamic load during the second week. Scale bar: (A, C) 1000 mm, (B, D) 500 mm.

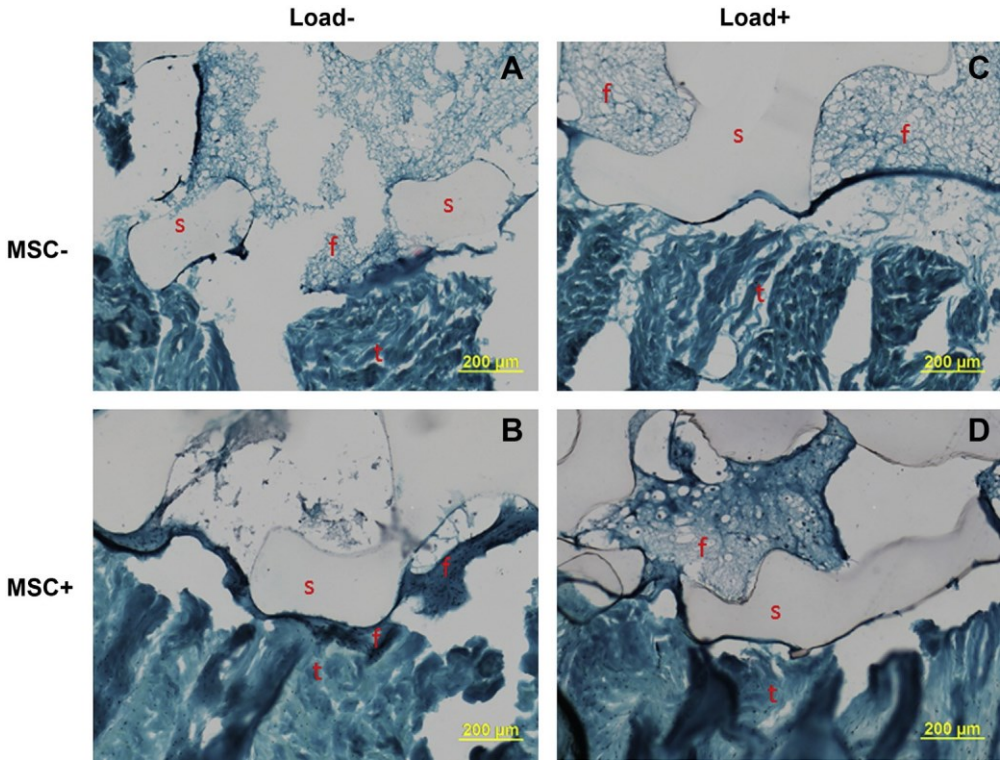

Fig. 5. Representative Safranin O/Fast Green stained sections of implant-AF interface in annulotomized IVD repaired with PTMC scaffold and PU membrane and cultured for 14 days with (C, D) or without (A, B) dynamic load during the second week, and with (B, D) or without (A, C) encapsulation of MSCs in the PTMC scaffold. Scale bar 200 mm. t - native disc tissue, s - PTMC scaffold fiber, f - fibrin gel seeded into PTMC scaffold.

3.4. Gene expression of native IVD tissue

COL1A2, COL2A1, ACAN and MMP13 gene expression levels in native disc tissue after 14 days of culture with (Load+) or without (Load−) dynamic load, and with (MSC+) or without (MSC−) MSC implantation were compared to the expression levels of healthy disc tissue from respective bovine tails before starting organ culture on day 0 (Fig. 6).

In both unloaded ($p < 0.01$) and loaded ($p < 0.05$) discs without MSC implantation, COL2 gene expression in the AF tissue next to PTMC scaffold decreased significantly compared with healthy AF tissue on day 0. With MSC implantation, COL2 gene expression remained comparable with day 0 healthy AF tissue. In unloaded discs, implantation of MSCs induced a 16.3-fold increase on COL2 gene expression in adjacent AF tissue (Load− MSC+ vs. Load− MSC−). In loaded discs, implantation of MSCs induced a 2.7-fold increase on COL2 gene expression in adjacent AF tissue (Load+ MSC+ vs. Load+ MSC−). There was a trend that MSCs implantation under dynamic load down-regulated MMP13 gene expression in the adjacent AF tissue to 13.9% compared with unloaded non MSC implanted discs.

In unloaded non MSC implanted discs, COL1 gene expression in the AF tissue opposite PTMC scaffold decreased significantly after 14 days of culture compared with healthy AF tissue on day 0 ($p < 0.05$). With implantation of MSCs and/or under dynamic load condition, COL1 gene expression remained comparable with day 0 healthy AF tissue. COL2 and MMP13 gene expression in AF tissue opposite PTMC scaffold also decreased significantly compared with healthy AF tissue on day 0.

After 14 days of culture, COL1 gene expression of NP tissue in unloaded non MSC implanted discs increased 8.0-fold compared with healthy NP tissue on day 0. Dynamic load down-regulated COL1 gene expression in NP tissue to 16.5% compared with unloaded discs (Load+ MSC− vs. Load− MSC−). COL2 gene expression of NP tissue in all groups decreased significantly compared with healthy NP tissue on day 0. Under dynamic load condition, implantation of MSCs induced a 3.1-fold increase on COL2 gene expression in NP tissue (Load+ MSC+ vs. Load+ MSC−). In MSC implanted discs, dynamic load showed a trend towards up-regulating ACAN gene expression in NP tissue (1.9-fold).

3.5. Biochemical analysis of PTMC scaffold

The DNA content of PTMC scaffolds seeded with MSCs was significantly higher compared with scaffolds without MSCs ($p < 0.001$). There was no difference in DNA content of PTMC scaffolds between loaded and unloaded samples (Fig. 7A).

The GAG content retained in the PTMC scaffolds was significantly higher in the unloaded samples compared with loaded samples (Fig. 7B, $p < 0.001$). On the other hand, there was no difference between PTMC scaffolds seeded with or without MSCs (Fig. 7B). Whereas GAG content within the conditioned media did not show any difference between groups during the first week of pre-culture, there was a significantly higher GAG amount in the conditioned media of the loaded discs compared with unloaded discs during one week of dynamic load ($p < 0.01$) (data not shown).

The OHP content accumulated within the scaffolds during 2 weeks of culture was very low (0.3–1.8 mg) and did not show significant differences between treatment groups.

3.6. Gene expression of hMSCs in PTMC scaffold within IVDs

ACAN and COL5A1 gene expression levels of hMSCs in PTMC scaffolds within discs cultured for 14 days were normalized to the expression levels of MSCs at day 0 of culture (after trypsinization and before 3D culture) (Fig. 7C). Compared with day 0, gene expression of

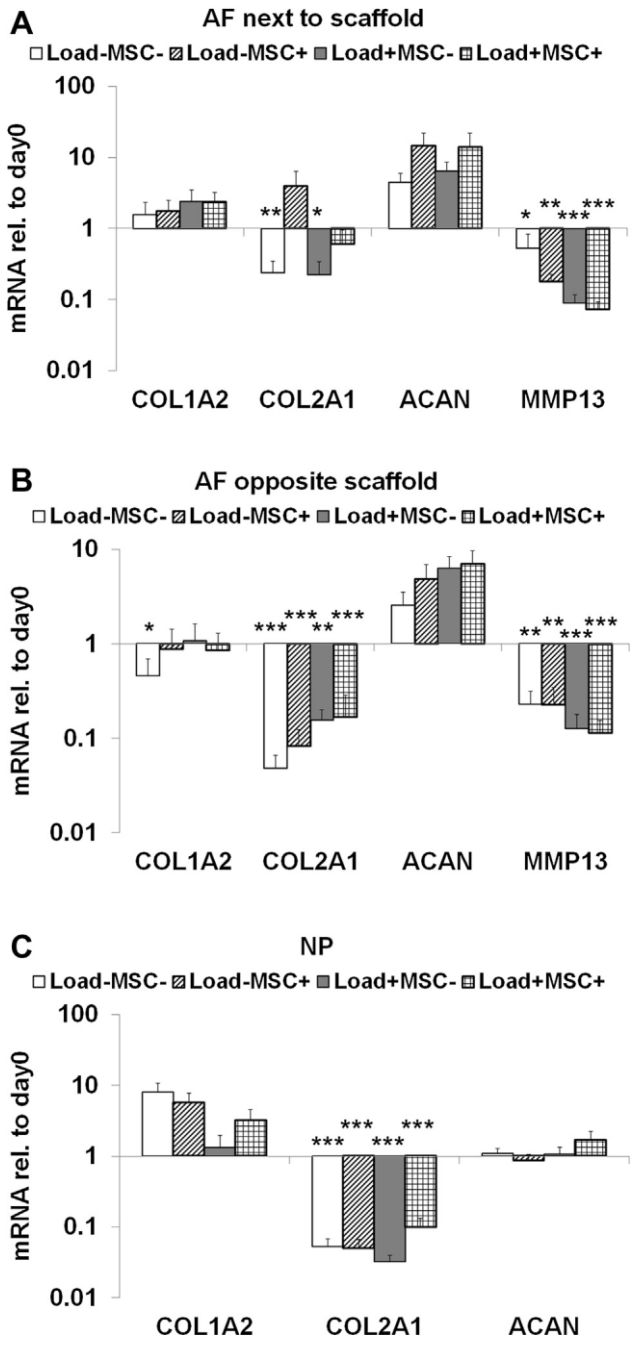

Fig. 6. Relative mRNA expression of COL1A2, COL2A1, ACAN and MMP13 in (A) adjacent AF, (B) distal AF, (C) NP of discs repaired with PTMC scaffold and PU membrane cultured for 14 days with (Loadþ) or without (Load—) dynamic load during the second week, and with (MSCþ) or without (MSC—) encapsulation of MSCs in the PTMC scaffold. Data were normalized to the expression level of healthy disc tissue from respective bovine tail before starting organ culture on day 0. MMP13 was undetectable in NP tissue. Mean þ SEM, n ¼ 15, *$p < 0.05$, **$p < 0.01$, ***$p < 0.001$ vs gene expression levels of healthy disc tissue from respective tails on day 0.

ACAN showed a trend of increase in unloaded discs (1.9-fold) after 14 days of culture. The COL5 gene expression of hMSCs increased 2.0-fold in unloaded discs and 2.7-fold in loaded discs.

4. Discussion

Effective biological AF repair is an unmet clinical demand for several indications: to prevent recurrent disc herniation; to prevent neural and vascular ingrowth associated with discogenic pain; to preserve the disc biology and biomechanics; to support NP replacement or NP regenerative therapy. In the current study, an organ culture model with dynamic load was used to assess the feasibility of scaffolds and MSC implantation for AF rupture repair. The reproducible organ culture AF defect model established in this study will allow the evaluation of various biomaterials and cell therapies before further preclinical animal studies.

Pilot experiments showed that press-fitted implants without closing were not able to withstand dynamic loading and were pressed out of the defect immediately after starting loading cycles. Therefore, a PU membrane, sutured onto the AF tissue, was used to cover the scaffold and seal the defect. After 14 days of assessment in organ culture under repetitive dynamic load, the sutured PU membrane retained the PTMC scaffold within the AF defect and no herniation of NP was observed (Fig. 4). Furthermore, the disc height profile of discs repaired with PTMC scaffolds was similar to intact discs and significantly improved compared with empty defect control discs (Fig. 3), which indicates that the mechanical function of annulotomized discs were partially restored by the implanted PTMC scaffolds and sutured PU membranes. These results suggest that the designed PTMC implant combined with a sutured PU membrane may be suitable as a basic prototype for AF rupture repair.

The induced AF injury in unloaded discs may suggest a degeneration process in both AF and NP tissues indicating by dedifferentiation of AF and NP cells. In AF tissue where collagen represents the dominant component of extracellular matrix [32], both COL1 and COL2 gene expression dropped significantly (Fig. 6). In NP tissue, COL1 gene expression showed a trend towards increase, while COL2 gene expression decreased significantly (Fig. 6). COL2 is the most affected gene, which indicates that the disc cells are undergoing a dedifferentiation process towards a fibrotic cell phenotype. A similar dedifferentiation process is often observed in *in vitro* cultures of AF cells [18] and NP cells [28].

It is well known that proper dynamic load is essential to maintain homeostasis and function of IVDs. In the current study, COL1 gene expression in AF tissue opposite PTMC scaffold decreased significantly in unloaded discs compared with day 0 healthy AF tissue, while repetitive dynamic load maintained COL1 gene expression in AF tissue and showed a trend towards down-regulation of MMP13 gene expression in AF tissue next to PTMC scaffold (Fig. 6). Furthermore, dynamic load down-regulated COL1 gene expression in NP tissue towards level more closed to the day 0 healthy NP tissue and showed a trend towards up-regulation of ACAN gene expression in NP tissue (Fig. 6). Previous *in vitro* [33,34] and *ex vivo* [35] studies have revealed similar results. Dynamic culture of AF cells *in vitro* enhanced extracellular matrix formation in silk scaffolds [33]. Cyclic tensile strain has shown to decrease MMP3 and ADAMTS4 gene expression of human AF cells cultured *in vitro* [34]. An organ culture study also showed that dynamic compression increased type II collagen, aggrecan and biglycan gene expression in both AF and NP tissues compared with free swelling culture conditions [35]. Taken together, our results corroborate that mechanical loading is crucial to mimic the physiological environment of IVDs in organ culture.

Implantation of MSCs into the AF defect was carried out by embedding them in a fibrin hydrogel, which has shown to improve cell seeding efficiency and cell distribution [36]. After 14 days of *in situ* culture with repetitive dynamic load, the implanted MSCs remained in the PTMC scaffolds, as indicated by histology staining (Fig. 5D) and DNA content measurement (Fig. 7A). COL5 gene expression of MSCs increased after 14 days of culture *in situ* (Fig. 7C). COL5 had been identified as a potential AF marker based

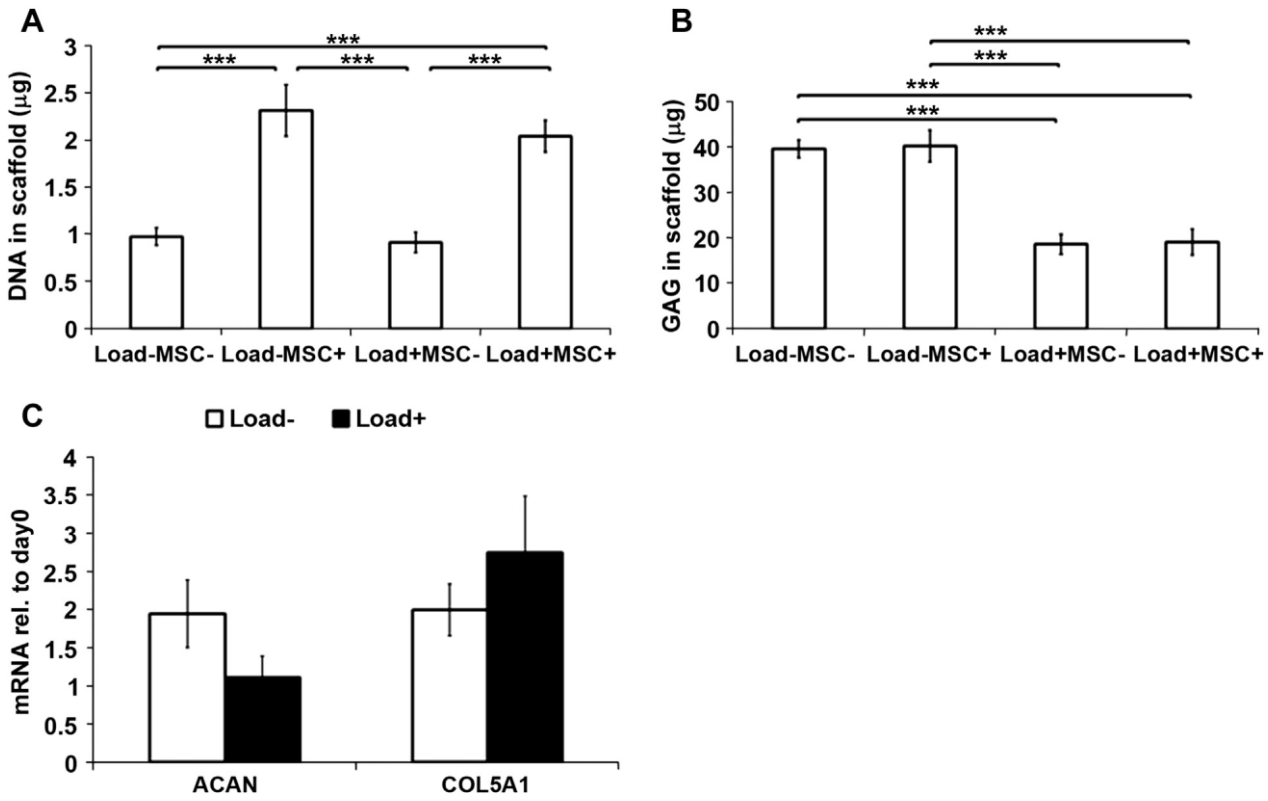

Fig. 7. (A) DNA, and (B) GAG content within PTMC scaffolds after 14 days culture in IVDs implanted either with (MSCþ) or without (MSC—) MSCs. After one week of pre-culture, discs were cultured with (Loadþ) or without (Load—) dynamic load in the second week. Mean ± SEM, $n = 7$, $^{***}p < 0.001$. (C) Relative mRNA expression of ACAN and COL5A1 of MSCs in PTMC scaffolds within IVDs after 14 days of culture with (Loadþ) or without (Load—) dynamic load during the second week. Data were normalized to the expression level of MSCs before implantation into IVDs on day 0. Mean ± SEM, $n = 8$.

on large scale gene expression profiling of AF cells in comparison to NP cells and chondrocytes [37,38]. These findings suggest that the implanted MSCs are able to adapt their phenotype during culture in IVDs. Longer term culture will be necessary to monitor MSC differentiation in more detail.

Nevertheless, implantation of MSCs showed a trend towards up-regulation of COL2 gene expression in the adjacent AF tissue and in the NP tissue (Fig. 6). Furthermore, implantation of MSCs under loaded condition showed a trend towards down-regulation of MMP13 gene expression in the adjacent AF tissue (Fig. 6). These results indicate that implantation of MSCs into IVDs with large AF defects may positively modulate cell phenotype of host disc tissue by up-regulating anabolic mechanisms and down-regulating catabolic mechanisms.

The above phenotype modulation observed in the implanted MSCs and adjacent AF and NP cells may be due to paracrine signals released by the two cell populations. A previous *in vitro* co-culture study of MSCs and AF cells indicated stimulatory effects on extracellular matrix synthesis [39]. MSCs have been shown to acquire a NP-like phenotype when directly co-cultured with NP cells *in vitro* [40,41]. The interaction between MSCs and degenerated NP cells also stimulated the NP cells to regain a non-degenerated phenotype [41].

Limitations of the PTMC scaffold/PU membrane device remain in the following 2 aspects: 1) the 4-points suture technique needs a large open space, which is difficult to achieve in mini-open surgery; 2) lack of sealing between the PU membrane and the PTMC scaffold leads to loss of extracellular matrix into the surrounding environment (Fig. 7B). To solve these problems, further development of the suture and/or sealing technique will be needed for eventual clinical application.

5. Conclusions

In the current study, PTMC scaffolds seeded with bone marrow derived MSCs in combination with an elastic PU membrane were assessed in an organ culture model for AF rupture repair. Designed PTMC implants combined with the sutured PU membrane restored the disc height of annulotomized discs, and prevented herniation of NP tissue into AF defect, hence may be suitable as an AF rupture closure device to reduce disc reherniation risk, stabilize disc biomechanics, and support NP repair strategies. In addition, implantation of MSCs shows potential of positively modulating cell phenotype of native disc tissue by up-regulating anabolic mechanisms and down-regulating catabolic mechanisms in host disc cells.

Acknowledgments

This study is funded by the Annulus Fibrosus Repair Collaborative Research Programme from AO Foundation. We thank Markus Glarner for his help with the poly(ester-urethane) synthesis, and Xu Chen for his help with the OHP assay. Fibrin components were kindly provided by Baxter Biosurgery, Vienna.

References

[1] Weber H. The natural history of disc herniation and the influence of intervention. Spine (Phila Pa 1976) 1994;19:2233e8.
[2] Katz JN. Lumbar disc disorders and low-back pain: socioeconomic factors and consequences. J Bone Jt Surg Am 2006;88(Suppl. 2):21e4.
[3] Asch HL, Lewis PJ, Moreland DB, Egnatchik JG, Yu YJ, Clabeaux DE, et al. Prospective multiple outcomes study of outpatient lumbar microdiscectomy: should 75 to 80% success rates be the norm? J Neurosurg 2002;96:34e44.

[4] McGirt MJ, Eustacchio S, Varga P, Vilendecic M, Trummer M, Gorensek M, et al. A prospective cohort study of close interval computed tomography and magnetic resonance imaging after primary lumbar discectomy: factors associated with recurrent disc herniation and disc height loss. Spine (Phila Pa 1976) 2009;34:2044e51.
[5] Carragee EJ, Han MY, Suen PW, Kim D. Clinical outcomes after lumbar discectomy for sciatica: the effects of fragment type and anular competence. J Bone Jt Surg Am 2003;85-A:102e8.
[6] Bailey A, Araghi A, Blumenthal S, Huffmon GV. Anular Repair Clinical Study G. Prospective, multicenter, randomized, controlled study of anular repair in lumbar discectomy: two-year follow-up. Spine (Phila Pa 1976) 2013;38:1161e9.
[7] Chiang CJ, Cheng CK, Sun JS, Liao CJ, Wang YH, Tsuang YH. The effect of a new anular repair after discectomy in intervertebral disc degeneration: an experimental study using a porcine spine model. Spine (Phila Pa 1976) 2011;36:761e9.
[8] Ahlgren BD, Lui W, Herkowitz HN, Panjabi MM, Guiboux JP. Effect of anular repair on the healing strength of the intervertebral disc: a sheep model. Spine (Phila Pa 1976) 2000;25:2165e70.
[9] Heuer F, Ulrich S, Claes L, Wilke HJ. Biomechanical evaluation of conventional anulus fibrosus closure methods required for nucleus replacement. Laboratory investigation. J Neurosurg Spine 2008;9:307e13.
[10] Grunert P, Borde BH, Hudson KD, Macielak MR, Bonassar LJ, Hartl R. Annular repair using high-density collagen gel: a rat-tail in vivo model. Spine (Phila Pa 1976) 2014;39:198e206.
[11] Guterl CC, Torre OM, Purmessur D, Dave K, Likhitpanichkul M, Hecht AC, et al. Characterization of mechanics and cytocompatibility of fibrin-genipin annulus fibrosus sealant with the addition of cell adhesion molecules. Tissue Eng Part A 2014.
[12] Sharifi S, Bulstra SK, Grijpma DW, Kuijer R. Treatment of the degenerated intervertebral disc; closure, repair and regeneration of the annulus fibrosus. J Tissue Eng Regen Med 2014.
[13] Guterl CC, See EY, Blanquer SB, Pandit A, Ferguson SJ, Benneker LM, et al. Challenges and strategies in the repair of ruptured annulus fibrosus. Eur Cell Mater 2013;25:1e21.
[14] Bron JL, Helder MN, Meisel HJ, Van Royen BJ, Smit TH. Repair, regenerative and supportive therapies of the annulus fibrosus: achievements and challenges. Eur Spine J 2009;18:301e13.
[15] Nerurkar NL, Baker BM, Sen S, Wible EE, Elliott DM, Mauck RL. Nanofibrous biologic laminates replicate the form and function of the annulus fibrosus. Nat Mater 2009;8:986e92.
[16] Blanquer SBG, Haimi SP, Poot AA, Grijpma DW. Effect of pore characteristics on mechanical properties and annulus fibrosus Cell seeding and proliferation in designed PTMC tissue engineering scaffolds. Macromol Symp 2013;334:75e81.
[17] Wilke HJ, Ressel L, Heuer F, Graf N, Rath S. Can prevention of a reherniation be investigated? Establishment of a herniation model and experiments with an anular closure device. Spine (Phila Pa 1976) 2013;38:E587e93.
[18] Wismer N, Grad S, Fortunato G, Ferguson SJ, Alini M, Eglin D. Biodegradable electrospun scaffolds for annulus fibrosus tissue engineering: effect of scaffold structure and composition on annulus fibrosus cells in vitro. Tissue Eng Part A 2014;20:672e82.
[19] Liebscher T, Haefeli M, Wuertz K, Nerlich AG, Boos N. Age-related variation in cell density of human lumbar intervertebral disc. Spine (Phila Pa 1976) 2011;36:153e9.
[20] Roughley PJ. Biology of intervertebral disc aging and degeneration: involvement of the extracellular matrix. Spine (Phila Pa 1976) 2004;29:2691e9.
[21] Gruber HE, Hoelscher G, Ingram JA, Hanley Jr EN. Culture of human anulus fibrosus cells on polyamide nanofibers: extracellular matrix production. Spine (Phila Pa 1976) 2009;34:4e9.
[22] See EY, Toh SL, Goh JC. Effects of radial compression on a novel simulated intervertebral disc-like assembly using bone marrow-derived mesenchymal stem cell cell-sheets for annulus fibrosus regeneration. Spine (Phila Pa 1976) 2011;36:1744e51.
[23] Driscoll TP, Nakasone RH, Szczesny SE, Elliott DM, Mauck RL. Biaxial mechanics and inter-lamellar shearing of stem-cell seeded electrospun angle-ply laminates for annulus fibrosus tissue engineering. J Orthop Res 2013;31:864e70.
[24] Nerurkar NL, Han W, Mauck RL, Elliott DM. Homologous structure-function relationships between native fibrocartilage and tissue engineered from MSC-seeded nanofibrous scaffolds. Biomaterials 2011;32:461e8.
[25] Nesti LJ, Li WJ, Shanti RM, Jiang YJ, Jackson W, Freedman BA, et al. Intervertebral disc tissue engineering using a novel hyaluronic acid-nanofibrous scaffold (HANFS) amalgam. Tissue Eng Part A 2008;14:1527e37.
[26] Gorna K, Gogolewski S. Biodegradable porous polyurethane scaffolds for tissue repair and regeneration. J Biomed Mater Res A 2006;79:128e38.
[27] Li Z, Kupcsik L, Yao SJ, Alini M, Stoddart MJ. Mechanical load modulates chondrogenesis of human mesenchymal stem cells through the TGF-beta pathway. J Cell Mol Med 2010;14:1338e46.
[28] Li Z, Kaplan KM, Wertzel A, Peroglio M, Amit B, Alini M, et al. Biomimetic fibrin-hyaluronan hydrogels for nucleus pulposus regeneration. Regen Med 2014;9:309e26.
[29] Illien-Junger S, Gantenbein-Ritter B, Grad S, Lezuo P, Ferguson SJ, Alini M, et al. The combined effects of limited nutrition and high-frequency loading on intervertebral discs with endplates. Spine (Phila Pa 1976) 2010;35:1744e52.
[30] Labarca C, Paigen K. A simple, rapid, and sensitive DNA assay procedure. Anal Biochem 1980;102:344e52.
[31] Farndale RW, Buttle DJ, Barrett AJ. Improved quantitation and discrimination of sulphated glycosaminoglycans by use of dimethylmethylene blue. Biochim Biophys Acta 1986;883:173e7.
[32] Pattappa G, Li Z, Peroglio M, Wismer N, Alini M, Grad S. Diversity of intervertebral disc cells: phenotype and function. J Anat 2012;221(6):480e96.
[33] Chang G, Kim HJ, Vunjak-Novakovic G, Kaplan DL, Kandel R. Enhancing annulus fibrosus tissue formation in porous silk scaffolds. J Biomed Mater Res A 2010;92:43e51.
[34] Gilbert HT, Hoyland JA, Millward-Sadler SJ. The response of human anulus fibrosus cells to cyclic tensile strain is frequency-dependent and altered with disc degeneration. Arthritis Rheum 2010;62:3385e94.
[35] Paul CP, Zuiderbaan HA, Zandieh Doulabi B, van der Veen AJ, van de Ven PM, Smit TH, et al. Simulated-physiological loading conditions preserve biological and mechanical properties of caprine lumbar intervertebral discs in ex vivo culture. PLoS One 2012;7:e33147.
[36] Lee CR, Grad S, Gorna K, Gogolewski S, Goessl A, Alini M. Fibrin-polyurethane composites for articular cartilage tissue engineering: a preliminary analysis. Tissue Eng 2005;11:1562e73.
[37] Clouet J, Grimandi G, Pot-Vaucel M, Masson M, Fellah HB, Guigand L, et al. Identification of phenotypic discriminating markers for intervertebral disc cells and articular chondrocytes. Rheumatology (Oxford) 2009;48:1447e50.
[38] Lee CR, Sakai D, Nakai T, Toyama K, Mochida J, Alini M, et al. A phenotypic comparison of intervertebral disc and articular cartilage cells in the rat. Eur Spine J 2007;16:2174e85.
[39] Le Visage C, Kim SW, Tateno K, Sieber AN, Kostuik JP, Leong KW. Interaction of human mesenchymal stem cells with disc cells: changes in extracellular matrix biosynthesis. Spine (Phila Pa 1976) 2006;31:2036e42.
[40] Richardson SM, Walker RV, Parker S, Rhodes NP, Hunt JA, Freemont AJ, et al. Intervertebral disc cell-mediated mesenchymal stem cell differentiation. Stem Cells 2006;24:707e16.
[41] Strassburg S, Richardson SM, Freemont AJ, Hoyland JA. Co-culture induces mesenchymal stem cell differentiation and modulation of the degenerate human nucleus pulposus cell phenotype. Regen Med 2010;5:701e11.